Chapter 6
A Natural Wind Tunnel

The solar wind has been used as a wind tunnel by Burlaga who, at the beginning of the 1990s, started to investigate anomalous fluctuations (Burlaga 1991a,c,b, 1995) as observed by measurements in the outer heliosphere by the Voyager spacecraft. In 1991, Marsch (1992), in a review on solar wind turbulence given at the *Solar Wind Seven* conference, underlined the importance of investigating scaling laws in the solar wind and we like to report his sentence: "The recent work by Burlaga (1991a,c) opens in my mind a very promising avenue to analyze and understand solar wind turbulence from a new theoretical vantage point. ... This approach may also be useful for MHD turbulence. Possible connections between intermittent turbulence and deterministic chaos have recently been investigated ... We are still waiting for applications of these modern concepts of chaos theory to solar wind MHD fluctuations." (cf. Marsch 1992, p. 503). A few years later Carbone (1993) and, independently, Biskamp (1993) faced the question of anomalous scaling from a theoretical point of view. More than 10 years later the investigation of statistical mechanics of MHD turbulence from one side, and of low-frequency solar wind turbulence on the other side, has produced a lot of papers, and is now mature enough to be tentatively presented in a more organic way.

6.1 Scaling Exponents of Structure Functions

The phenomenology of turbulence developed by Kolmogorov (1941) deals with some statistical hypotheses for fluctuations. The famous footnote remark by Landau (Landau and Lifshitz 1971) pointed out a defect in the Kolmogorov theory, namely the fact that the theory does not take proper account of spatial fluctuations of local dissipation rate (Frisch 1995). This led different authors to investigate the features related to scaling laws of fluctuations and, in particular, to investigate the departure from the Kolmogorov's linear scaling of the structure functions (cf. Sect. 2.8). An

R. Bruno, V. Carbone, *Turbulence in the Solar Wind*, Lecture Notes in Physics 928, DOI 10.1007/978-3-319-43440-7_6

up-to-date comprehensive review of these theoretical efforts can be found in the book by Frisch (1995).

Here we are interested in understanding what we can learn from solar wind turbulence about the basic features of scaling laws for fluctuations. We use velocity and magnetic fields time series, and we investigate the scaling behavior of the high-order moments of stochastic variables defined as variations of fields separated by a time[1] interval τ. First of all, it is worthwhile to remark that scaling laws and, in particular, the exact relation (2.41) which defines the inertial range in fluid flows, is valid for longitudinal (streamwise) fluctuations. In common fluid flows the Kolmogorov linear scaling law is compared with the moments of longitudinal velocity differences. In the same way for the solar wind turbulence we investigate the scaling behavior of $\Delta u_\tau = u(t+\tau) - u(t)$, where $u(t)$ represents the component of the velocity field along the radial direction. As far as the magnetic differences are concerned $\Delta b_\tau = B(t+\tau) - B(t)$, we are free for different choices and, in some sense, this is more interesting from an experimental point of view. We can use the reference system where $B(t)$ represents the magnetic field projected along the radial direction, or the system where $B(t)$ represents the magnetic field along the local background magnetic field, or $B(t)$ represents the field along the minimum variance direction. As a different case we can simply investigate the scaling behavior of the fluctuations of the magnetic field intensity.

Let us consider the pth moment of both absolute values[2] of velocity fluctuations $R_p(\tau) = \langle |\Delta u_\tau|^p \rangle$ and magnetic fluctuations $S_p(\tau) = \langle |\Delta b_\tau|^p \rangle$, also called pth order structure function in literature (brackets being time average). Here we use magnetic fluctuations across structures at intervals τ calculated by using the magnetic field intensity. Typical structure functions of magnetic field fluctuations, for two different values of p, for both a slow wind and a fast wind at 0.9 AU, are shown in Fig. 6.1. The magnetic field we used is that measured by Helios 2 spacecraft. Structure functions calculated for the velocity fields have roughly the same shape. Looking at these figures the typical scaling features of turbulence can be observed. Starting from low values at small scales, the structure functions increase towards a region where $S_p \to$ const. at the largest scales. This means that at these scales the field fluctuations are uncorrelated. A kind of "inertial range", that is a region of intermediate scales τ

[1] Since the solar wind moves at supersonic speed V_{sw}, the usual Taylor's hypothesis is verified, and we can get information on spatial scaling laws ℓ by using time differences $\tau = \ell / V_{sw}$.

[2] Note that, according to the occurrence of the Yaglom's law, that is a third-order moment is different from zero, the fluctuations at a given scale in the inertial range must present some non-Gaussian features. From this point of view the calculation of structure functions with the absolute value is unappropriate because in this way we risk to cancel out non-Gaussian features. Namely we symmetrize the probability density functions of fluctuations. However, in general, the number of points at disposal is much lower than required for a robust estimate of odd structure functions, even in usual fluid flows. Then, as usually, we will obtain structure functions by taking the absolute value, even if some care must be taken in certain conclusions which can be found in literature.

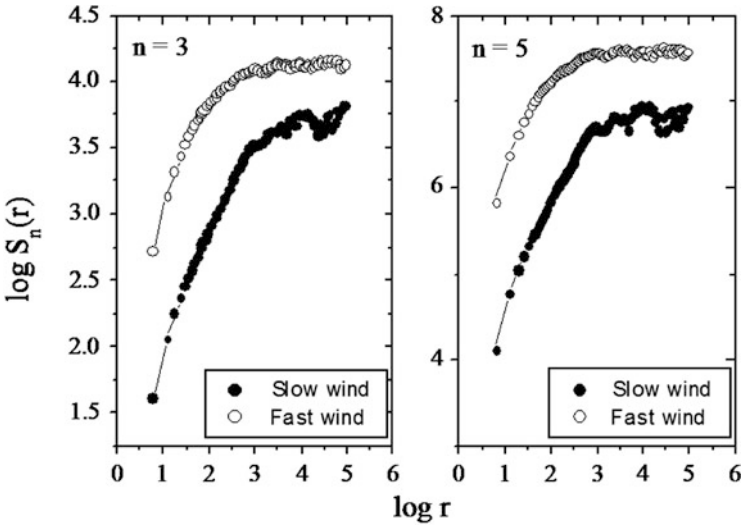

Fig. 6.1 Structure functions for the magnetic field intensity $S_n(r)$ for two different orders, $n = 3$ and $n = 5$, for both slow wind and fast wind, as a function of the time scale r. Data come from Helios 2 spacecraft at 0.9 AU

where a power law can be recognized for both

$$R_p(\tau) = \langle |\Delta u_\tau|^p \rangle \sim \tau^{\zeta_p}$$
$$S_p(\tau) = \langle |\Delta b_\tau|^p \rangle \sim \tau^{\xi_p} \tag{6.1}$$

is more or less visible only for the slow wind. In this range correlations exists, and we can obtain the scaling exponents ζ_p and ξ_p through a simple linear fit.

Since as we have seen, Yaglom's law is observed only in some few samples, the inertial range in the whole solar wind is not well defined. A look at Fig. 6.1 clearly shows that we are in a situation similar to a low-Reynolds number fluid flow. In order to compare scaling exponents of the solar wind turbulent fluctuations with other experiments, it is perhaps better to try to recover exponents using the Extended Self-Similarity (ESS), introduced some time ago by Benzi et al. (1993), and used here as a tool to determine relative scaling exponents. In the fluid-like case, the third-order structure function can be regarded as a generalized scaling using the inverse of Eq. (2.42) or of Eq. (2.41) (Politano et al. 1998). Then, we can plot the pth order structure function vs. the third-order one to recover at least relative scaling exponents ζ_p/ζ_3 and ξ_p/ξ_3 (6.1). Quite surprisingly (see Fig. 6.2), we find that the range where a power law can be recovered extends well beyond the inertial range, covering almost all the experimental range. In the fluid case the scaling exponents which can be obtained through ESS at low or moderate Reynolds numbers, coincide with the scaling exponents obtained for high Reynolds, where the inertial range is very well defined (Benzi et al. 1993). This is due to the fact that, since by definition

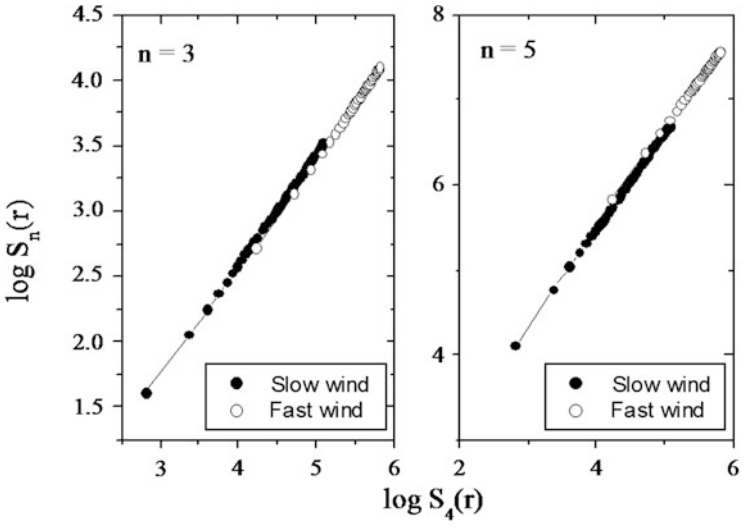

Fig. 6.2 Structure functions $S_n(r)$ for two different orders, $n = 3$ and $n = 5$, for both slow wind and high wind, as a function of the fourth-order structure function $S_4(r)$. Data come from Helios 2 spacecraft at 0.9 AU

$\zeta_3 = 1$ in the inertial range (Frisch 1995), whatever its extension might be. In our case scaling exponents obtained through ESS can be used as a surrogate, since we cannot be sure that an inertial range exists.

It is worthwhile to remark (as shown in Fig. 6.2) that we can introduce a general scaling relation between the qth order velocity structure function and the pth order structure function, with a relative scaling exponent $\alpha_p(q)$. It has been found that this relation becomes an exact relation

$$S_q(r) = \left[S_p(r)\right]^{\alpha_p(q)},$$

when the velocity structure functions are normalized to the average velocity within each period used to calculate the structure function (Carbone et al. 1996a). This is very interesting because it implies that the above relationship is satisfied by the following probability distribution function, if we assume that odd moments are much smaller than the even ones (Carbone et al. 1996a):

$$PDF(\Delta u_\tau) = \int_{-\infty}^{\infty} dk\, e^{ik\Delta u_\tau} \sum_{q=0}^{\infty} \frac{(ik)^{2q}}{2\pi(2q)!} \left[S_p(\tau)\right]^{\alpha_p(2q)}. \tag{6.2}$$

That is, for each scale τ the knowledge of the relative scaling exponents $\alpha_p(q)$ completely determines the probability distribution of velocity differences as a function of a single parameter $S_p(\tau)$.

Table 6.1 Scaling exponents for velocity ζ_p and magnetic ξ_p variables calculated through ESS

p	ζ_p	ξ_p	$u(t)$ (fluid)	$T(t)$ (fluid)
1	0.37 ± 0.06	0.56 ± 0.06	0.37	0.61
2	0.70 ± 0.05	0.83 ± 0.05	0.70	0.85
3	1.00	1.00	1.00	1.00
4	1.28 ± 0.02	1.14 ± 0.02	1.28	1.12
5	1.54 ± 0.03	1.25 ± 0.03	1.54	1.21
6	1.79 ± 0.05	1.35 ± 0.05	1.78	1.38

Errors represent the standard deviations of the linear fitting. The data used comes from a turbulent sample of slow wind at 0.9 AU from Helios 2 spacecraft. As a comparison we show the normalized scaling exponents of structure functions calculated in a wind tunnel on Earth (Ruíz-Chavarría et al. 1995) for velocity and temperature. The temperature is a passive scalar in this experiment

Relative scaling exponents, calculated by using data coming from Helios 2 at 0.9 AU, are reported in Table 6.1. As it can be seen, two main features can be noted:

1. There is a significant departure from the Kolmogorov linear scaling, that is, real scaling exponents are anomalous and seem to be non-linear functions of p, say $\zeta_p/\zeta_3 > p/3$ for $p < 3$, while $\zeta_p/\zeta_3 < p/3$ for $p > 3$. The same behavior can be observed for ξ_p/ξ_3. In Table 6.1 we report also the scaling exponents obtained in usual fluid flows for velocity and temperature, the latter being a passive scalar. Scaling exponents for velocity field are similar to scaling exponents obtained in turbulent flows on Earth, showing a kind of universality in the anomaly. This effect is commonly attributed to the phenomenon of *intermittency* in fully developed turbulence (Frisch 1995). Turbulence in the solar wind is intermittent, just like its fluid counterpart on Earth.
2. The degree of intermittency is measured through the distance between the curve ζ_p/ζ_3 and the linear scaling $p/3$. It can be seen that the magnetic field is more intermittent than the velocity field. The same difference is observed between the velocity field and a passive scalar (in our case the temperature) in ordinary fluid flows (Ruíz-Chavarría et al. 1995). That is the magnetic field, as long as intermittency properties are concerned, has the same scaling laws of a passive field. Of course *this does not mean that the magnetic field plays the same role as a passive field.* Statistical properties are in general different from dynamical properties.

In Table 6.1 we show scaling exponents up to the sixth order. Actually, a question concerns the validation of high-order moments estimates, say the maximum value of the order p which can be determined with a finite number of points of our dataset. As the value of p increases, we need an increasing number of points for an optimal determination of the structure function (Tennekes and Wyngaard 1972). Anomalous

scaling laws are generated by rare and intense events due to singularities in the gradients: the higher their intensity the more rare these events are. Of course, when the data set has a finite extent, the probability to get singularities stronger than a certain value approaches zero. In that case, scaling exponents ζ_p of order higher than a certain value become linear functions of p. Actually, the structure function $S_p(\tau)$ depends on the probability distribution function $\mathrm{PDF}(\Delta u_\tau)$ through

$$S_p(\tau) = \int \Delta u_\tau^p \, \mathrm{PDF}(\delta u_\tau) \, d\Delta u_\tau$$

and, the function S_p is determined only when the integral converges. As p increases, the function $F_p(\delta u_\tau) = \Delta u_\tau^p \, \mathrm{PDF}(\Delta u_\tau)$ becomes more and more disturbed, with some spikes, so that the integral becomes more and more undefined, as can be seen for example in Fig. 1 of the paper by Dudok de Wit (2004). A simple calculation (Dudok de Wit 2004) for the maximum value of the order p_m which can reliably be estimated with a given number N of points in the dataset, gives the empirical criterion $p_m \simeq \log N$. Structure functions of order $p > p_m$ cannot be determined accurately.

Only few large structures are enough to generate the anomalous scaling laws. In fact, as shown by Salem et al. (2009), by suppressing through wavelets analysis just a few percentage of large structures on all scales, the scaling exponents become linear functions of p, respectively $p/4$ and $p/3$ for the kinetic and magnetic fields.

As far as a comparison between different plasmas is concerned, the scaling exponents of magnetic structure functions, obtained from laboratory plasma experiments of a Reversed-Field Pinch at different distances from the external wall (Carbone et al. 2000) are shown in Table 6.2. In laboratory plasmas it is difficult to measure all the components of the vector field at the same time, thus, here we show only the scaling exponents obtained using magnetic field differences $B_r(t+\tau) - B_r(t)$ calculated from the radial component in a toroidal device where the z-axis is directed along the axis of the torus. As it can be seen, intermittency in magnetic turbulence is not so strong as it appears to be in the solar wind, actually the degree of intermittency

Table 6.2 Normalized scaling exponents ξ_p/ξ_3 for radial magnetic fluctuations in a laboratory plasma, as measured at different distances a/R ($R \simeq 0.45$ cm being the minor radius of the torus in the experiment) from the external wall

p	$a/R = 0.96$	$a/R = 0.93$	$a/R = 0.90$	$a/R = 0.86$
1	0.39 ± 0.01	0.38 ± 0.01	0.37 ± 0.01	0.36 ± 0.01
2	0.74 ± 0.01	0.73 ± 0.02	0.71 ± 0.01	0.70 ± 0.01
3	1.00	1.00	1.00	1.00
4	1.20 ± 0.02	1.24 ± 0.02	1.27 ± 0.01	1.28 ± 0.01
5	1.32 ± 0.03	1.41 ± 0.03	1.51 ± 0.03	1.55 ± 0.03
6	1.38 ± 0.04	1.50 ± 0.04	1.71 ± 0.03	1.78 ± 0.04

Errors represent the standard deviations of the linear fitting. Scaling exponents have been obtained using the ESS

Table 6.3 Normalized scaling exponents ξ_p/ξ_3 for Alfvénic, velocity, and magnetic fluctuations obtained from data of high resolution 2D MHD numerical simulations

p	Z^+	Z^-	v	B
1	0.36 ± 0.06	0.56 ± 0.06	0.37 ± 0.01	0.46 ± 0.02
2	0.70 ± 0.05	0.83 ± 0.05	0.70 ± 0.01	0.78 ± 0.01
3	1.00	1.00	1.00	1.00
4	1.28 ± 0.02	1.14 ± 0.02	1.28 ± 0.02	1.18 ± 0.02
5	1.53 ± 0.03	1.25 ± 0.03	1.54 ± 0.03	1.31 ± 0.03
6	1.79 ± 0.05	1.35 ± 0.05	1.78 ± 0.05	1.40 ± 0.03

Scaling exponents have been calculated from spatial fluctuations; different times, in the statistically stationary state, have been used to improve statistics. The scaling exponents have been calculated by ESS using Eq. (2.41) as characteristic scale rather than the third-order structure function (cf. Politano et al. 1998, for details

increases when going toward the external wall. This last feature appears to be similar to what is currently observed in channel flows, where intermittency also increases when going towards the external wall (Pope 2000).

Scaling exponents of structure functions for Alfvén variables, velocity, and magnetic variables have been calculated also for high resolution 2D incompressible MHD numerical simulations (Politano et al. 1998). In this case, we are freed from the constraint of the Taylor hypothesis when calculating the fluctuations at a given scale. From 2D simulations we recover the fields $\mathbf{u}(\mathbf{r}, t)$ and $\mathbf{b}(\mathbf{r}, t)$ at some fixed times. We calculate the longitudinal fluctuations directly in space at a fixed time, namely $\Delta u_\ell = [\mathbf{u}(\mathbf{r} + \ell, t) - \mathbf{u}(\mathbf{r}, t)] \cdot \ell/\ell$ (the same are made for different fields, namely the magnetic field or the Elsässer fields). Finally, averaging both in space and time, we calculate the scaling exponents through the structure functions. These scaling exponents are reported in Table 6.3. Note that, even in numerical simulations, intermittency for magnetic variables is stronger than for the velocity field.

6.2 Probability Distribution Functions and Self-Similarity of Fluctuations

The presence of scaling laws for fluctuations is a signature of the presence of self-similarity in the phenomenon. A given observable $u(\ell)$, which depends on a scaling variable ℓ, is invariant with respect to the scaling relation $\ell \to \lambda\ell$, when there exists a parameter $\mu(\lambda)$ such that $u(\ell) = \mu(\lambda)u(\lambda\ell)$. The solution of this last relation is a power law $u(\ell) = C\ell^h$, where the scaling exponent is $h = -\log_\lambda \mu$.

Since, as we have just seen, turbulence is characterized by scaling laws, this must be a signature of self-similarity for fluctuations. Let us see what this means. Let us consider fluctuations at two different scales, namely $\Delta z_\ell^\pm$ and $\Delta z_{\lambda\ell}^\pm$. Their ratio $\Delta z_{\lambda\ell}^\pm / \Delta z_\ell^\pm \sim \lambda^h$ depends only on the value of h, and this should imply that fluctuations are self-similar. This means that PDFs are related through

$$P(\Delta z_{\lambda\ell}^\pm) = \mathrm{PDF}(\lambda^h \Delta z_\ell^\pm).$$

Let us consider the normalized variables

$$y_\ell^\pm = \frac{\Delta z_\ell^\pm}{\langle (\Delta z_\ell^\pm)^2 \rangle^{1/2}}.$$

When h is unique or in a pure self-similar situation, PDFs are related through $P(y_\ell^\pm) = \mathrm{PDF}(y_{\lambda\ell}^\pm)$, say by changing scale PDFs coincide.

The PDFs relative to the normalized magnetic fluctuations $\delta b_\tau = \Delta b_\tau / \langle \Delta b_\tau^2 \rangle^{1/2}$, at three different scales τ, are shown in Fig. 6.3. It appears evident that the global self-similarity in real turbulence is broken. PDFs do not coincide at different scales,

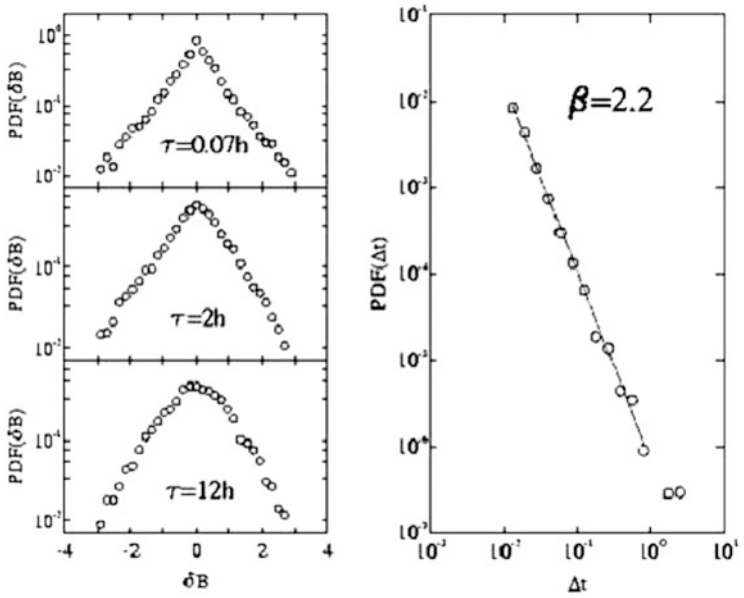

Fig. 6.3 *Left panel*: normalized PDFs for the magnetic fluctuations observed in the solar wind turbulence by using Helios data. *Right panel*: distribution function of waiting times Δt between structures at the smallest scale. The parameter β is the scaling exponent of the scaling relation $\mathrm{PDF}(\Delta t) \sim \Delta t^{-\beta}$ for the distribution function of waiting times

rather their shape seems to depend on the scale τ. In particular, at large scales PDFs seem to be almost Gaussian, but they become more and more stretched as τ decreases. At the smallest scale PDFs are stretched exponentials. This scaling dependence of PDFs is a different way to say that scaling exponents of fluctuations are anomalous, or can be taken as a different definition of intermittency. Note that the wings of PDFs are higher than those of a Gaussian function. This implies that intense fluctuations have a probability of occurrence higher than that they should have if they were Gaussianly distributed. Said differently, intense stochastic fluctuations are less rare than we should expect from the point of view of a Gaussian approach to the statistics. These fluctuations play a key role in the statistics of turbulence. The same statistical behavior can be found in different experiments related to the study of the atmosphere (see Fig. 6.4) and the laboratory plasma (see Fig. 6.5).

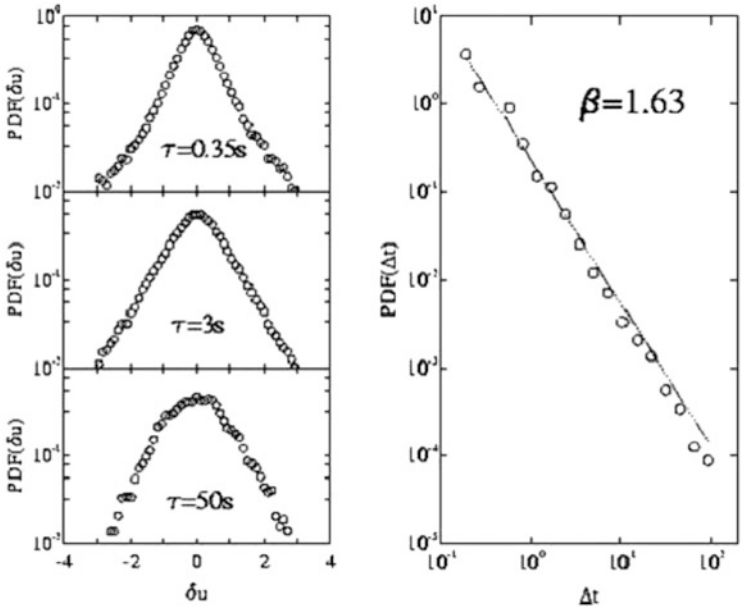

Fig. 6.4 *Left panel*: normalized PDFs of velocity fluctuations in atmospheric turbulence. *Right panel*: distribution function of waiting times Δt between structures at the smallest scale. The parameter β is the scaling exponent of the scaling relation $\mathrm{PDF}(\Delta t) \sim \Delta t^{-\beta}$ for the distribution function of waiting times. The turbulent samples have been collected above a grass-covered forest clearing at 5 m above the ground surface and at a sampling rate of 56 Hz (Katul et al. 1997)

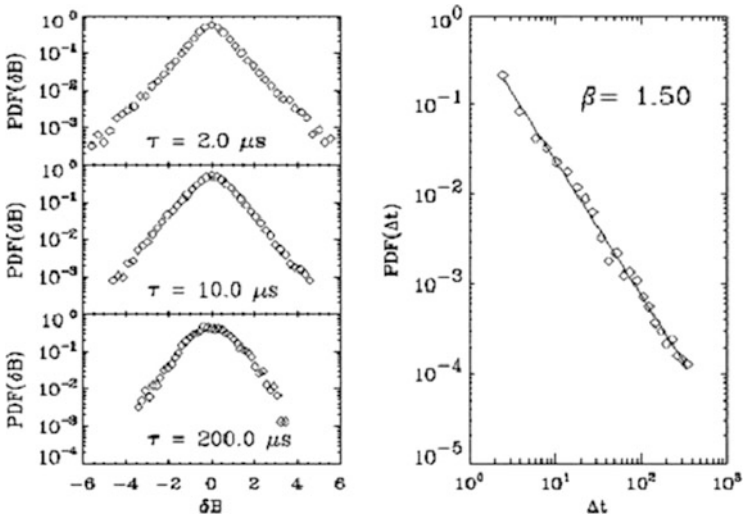

Fig. 6.5 *Left panel*: normalized PDFs of the radial magnetic field collected in RFX magnetic turbulence (Carbone et al. 2000). *Right panel*: distribution function of waiting times Δt between structures at the smallest scale. The parameter β is the scaling exponent of the scaling relation $\mathrm{PDF}(\Delta t) \sim \Delta t^{-\beta}$ for the distribution function of waiting times

6.3 What is Intermittent in the Solar Wind Turbulence? The Multifractal Approach

Time dependence of Δu_τ and Δb_τ for three different scales τ is shown in Figs. 6.6 and 6.7, respectively. These plots show that, as τ becomes small, intense fluctuations become more and more important, and they dominate the statistics. Fluctuations at large scales appear to be smooth while, as the scale becomes smaller, intense fluctuations becomes visible. These dominating fluctuations represent relatively rare events. Actually, at the smallest scales, the time behavior of both Δu_τ and Δb_τ is dominated by regions where fluctuations are low, in between regions where fluctuations are intense and turbulent activity is very high. Of course, this behavior cannot be described by a global self-similar behavior. Allowing the scaling laws to vary with the region of turbulence we are investigating would be more convincing.

The behavior we have just described is at the heart of the multifractal approach to turbulence (Frisch 1995). In that description of turbulence, even if the small scales of fluid flow cannot be globally self-similar, self-similarity can be reintroduced as a local property. In the multifractal description it is conjectured that turbulent flows can be made by an infinite set of points $S_h(\mathbf{r})$, each set being characterized by a scaling law $\Delta Z_\ell^\pm \sim \ell^{h(\mathbf{r})}$, that is, the scaling exponent can depend on the position $\mathbf{r}$. The usual dimension of that set is then not constant, but depends on the local value of h, and is quoted as $D(h)$ in literature.

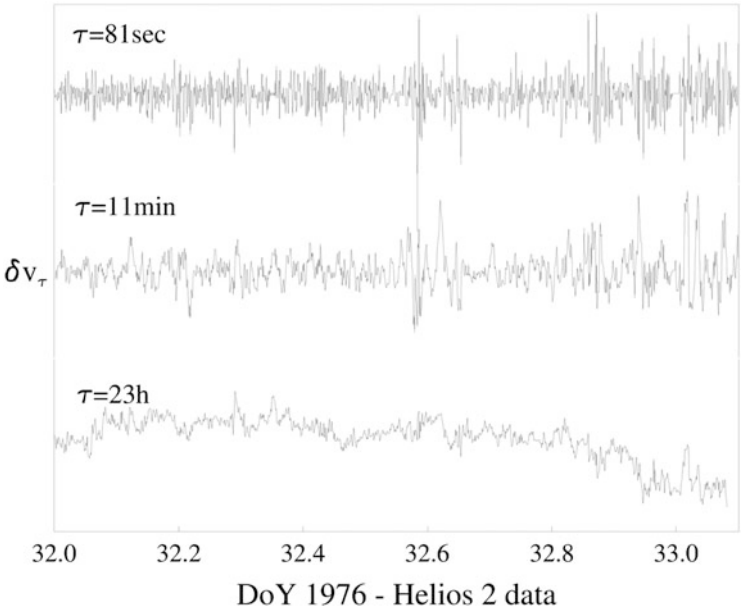

Fig. 6.6 Differences for the longitudinal velocity $\delta u_\tau = u(t+\tau) - u(t)$ at three different scales τ, as shown in the figure

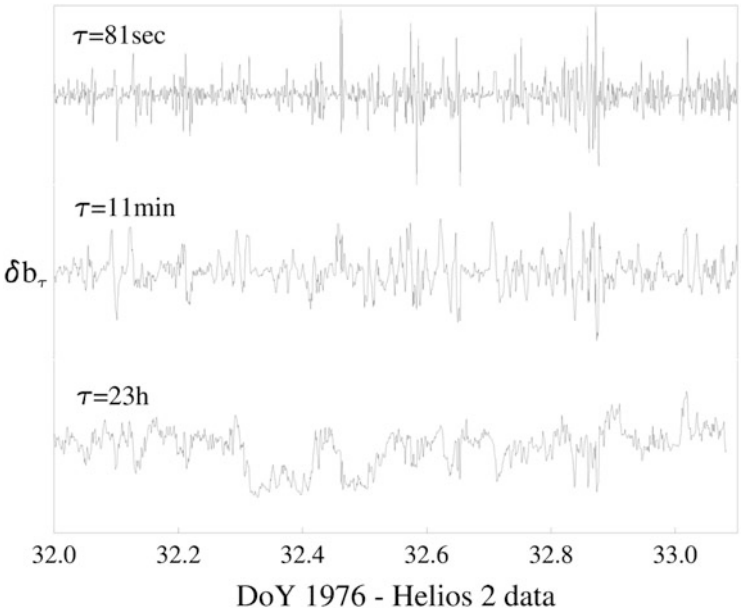

Fig. 6.7 Differences for the magnetic intensity $\Delta b_\tau = B(t+\tau) - B(t)$ at three different scales τ, as shown in the figure

Then, the probability of occurrence of a given fluctuation can be calculated through the weight the fluctuation assumes within the whole flow, i.e.,

$$P(\Delta Z_\ell^\pm) \sim (\Delta Z_\ell^\pm)^h \times \text{volume occupied by fluctuations},$$

and the pth order structure function is immediately written through the integral over all (continuous) values of h weighted by a smooth function $\mu(h) \sim 0(1)$, i.e.,

$$S_p(\ell) = \int \mu(h)(\Delta Z_\ell^\pm)^{ph}(\Delta Z_\ell^\pm)^{3-D(h)}dh.$$

A moment of reflection allows us to realize that in the limit $\ell \to 0$ the integral is dominated by the minimum value (over h) of the exponent and, as shown by Frisch (1995), the integral can be formally solved using the usual saddle-point method. The scaling exponents of the structure function can then be written as

$$\zeta_p = \min_h[ph + 3 - D(h)].$$

In this way, the departure of ζ_p from the linear Kolmogorov scaling and thus intermittency, can be characterized by the continuous changing of $D(h)$ as h varies. That is, as p varies we are probing regions of fluid where even more rare and intense events exist. These regions are characterized by small values of h, that is, by stronger singularities of the gradient of the field.

Owing to the famous Landau footnote on the fact that fluctuations of the energy transfer rate must be taken into account in determining the statistics of turbulence, people tried to interpret the non-linear energy cascade typical of turbulence theory, within a geometrical framework. The old Richardson's picture of the turbulent behavior as the result of a hierarchy of eddies at different scales has been modified and, as realized by Kraichnan (1974), once we leave the idea of a constant energy cascade rate we open a "Pandora's box" of possibilities for modeling the energy cascade. By looking at scaling laws for $\Delta z_\ell^\pm$ and introducing the scaling exponents for the energy transfer rate $\langle \epsilon_\ell^p \rangle \sim r^{\tau_p}$, it can be found that $\zeta_p = p/m + \tau_{p/m}$ (being $m = 3$ when the Kolmogorov-like phenomenology is taken into account, or $m = 4$ when the Iroshnikov-Kraichnan phenomenology holds). In this way the intermittency correction are determined by a cascade model for the energy transfer rate. When τ_p is a non-linear function of p, the energy transfer rate can be described within the multifractal geometry (see, e.g., Meneveau 1991, and references therein) characterized by the generalized dimensions $D_p = 1 - \tau_p/(p-1)$ (Hentschel and Procaccia 1983). The scaling exponents of the structure functions are then related to D_p by

$$\zeta_p = \left(\frac{p}{m} - 1\right) D_{p/m} + 1.$$

The correction to the linear scaling p/m is positive for $p < m$, negative for $p > m$, and zero for $p = m$. A fractal behavior where $D_p = \text{const.} < 1$ gives a linear correction with a slope different from $1/m$.

6.4 Fragmentation Models for the Energy Transfer Rate

Cascade models view turbulence as a collection of fragments at a given scale ℓ, which results from the fragmentation of structures at the scale $\ell' > \ell$, down to the dissipative scale (Novikov 1969). Sophisticated statistics are applied to obtain scaling exponents ζ_p for the pth order structure function.

The starting point of fragmentation models is the old β-model, a "pedagogical" fractal model introduced by Frisch et al. (1978) to account for the modification of the cascade in a simple way. In this model, the cascade is realized through the conjecture that active eddies and non-active eddies are present at each scale, the space-filling factor for the fragments being fixed for each scale. Since it is a fractal model, the β-model gives a *linear* modification to ζ_p. This can account for a fit on the data, as far as small values of p are concerned. However, the whole curve ζ_p is clearly nonlinear, and a multifractal approach is needed.

The random-β model (Benzi et al. 1984), a multifractal modification of the β-model, can be derived by invoking that the space-filling factor for the fragments at a given scale in the energy cascade is not fixed, but is given by a random variable β. The probability of occurrence of a given β is assumed to be a bimodal distribution where the eddies fragmentation process generates either space-filling eddies with probability ξ or planar sheets with probability $(1-\xi)$ (for conservation $0 \leq \xi \leq 1$). It can be found that

$$\zeta_p = \frac{p}{m} - \log_2\left[1 - \xi + \xi 2^{p/m-1}\right], \tag{6.3}$$

where the free parameter ξ can be fixed through a fit on the data.

The p-model (Meneveau 1991; Carbone 1993) consists in an eddies fragmentation process described by a two-scale Cantor set with equal partition intervals. An eddy at the scale ℓ, with an energy derived from the transfer rate ϵ_r, breaks down into two eddies at the scale $\ell/2$, with energies $\mu\epsilon_r$ and $(1-\mu)\epsilon_r$. The parameter $0.5 \leq \mu \leq 1$ is not defined by the model, but is fixed from the experimental data. The model gives

$$\zeta_p = 1 - \log_2\left[\mu^{p/m} + (1-\mu)^{p/m}\right]. \tag{6.4}$$

In the model by She and Leveque (see, e.g., She and Leveque 1994; Politano and Pouquet 1998) one assumes an infinite hierarchy for the moments of the energy transfer rates, leading to $\epsilon_r^{(p+1)} \sim [\epsilon_r^{(p)}]^{\beta}[\epsilon_r^{(\infty)}]^{1-\beta}$, and a divergent scaling law for

the infinite-order moment $\epsilon_r^{(\infty)} \sim r^{-x}$, which describes the most singular structures within the flow. The model reads

$$\zeta_p = \frac{p}{m}(1-x) + \mathrm{C}\left[1 - \left(1 - \frac{x}{\mathrm{C}}\right)^{p/m}\right]. \tag{6.5}$$

The parameter $\mathrm{C} = x/(1-\beta)$ is identified as the codimension of the most singular structures. In the standard MHD case (Politano and Pouquet 1995) $x = \beta = 1/2$, so that $\mathrm{C} = 1$, that is, the most singular dissipative structures are planar sheets. On the contrary, in fluid flows $\mathrm{C} = 2$ and the most dissipative structures are filaments. The large p behavior of the p-model is given by $\zeta_p \sim (p/m)\log_2(1/\mu) + 1$, so that Eqs. (6.4) and (6.5) give the same results providing $\mu \simeq 2^{-x}$. As shown by Carbone et al. (1996b) all models are able to capture intermittency of fluctuations in the solar wind. The agreement between the curves ζ_p and normalized scaling exponents is excellent, and this means that we realistically cannot discriminate between the models we reported above. The main problem is that all models are based on a conjecture which gives a curve ζ_p as a function of a single free parameter, and that curve is able to fit the smooth observed behavior of ζ_p. Statistics cannot prove, just disprove. We can distinguish between the fractal model and multifractal models, but we cannot realistically distinguish among the various multifractal models.

6.5 A Model for the Departure from Self-Similarity

Besides the idea of self-similarity underlying the process of energy cascade in turbulence, a different point of view can be introduced. The idea is to characterize the behavior of the PDFs through the scaling laws of the parameters, which describe how the shape of the PDFs changes when going towards small scales. The model, originally introduced by Castaing et al. (2001), is based on a multiplicative process describing the cascade. In its simplest form the model can be introduced by saying that PDFs of increments $\delta Z_\ell^\pm$, at a given scale, are made as a sum of Gaussian distributions with different widths $\sigma = \langle(\delta Z_\ell^\pm)^2\rangle^{1/2}$. The distribution of widths is given by $G_\lambda(\sigma)$, namely

$$P(\delta Z_\ell^\pm) = \frac{1}{2\pi}\int_0^\infty G_\lambda(\sigma)\exp\left(-\frac{(\delta Z_\ell^\pm)^2}{2\sigma^2}\right)\frac{d\sigma}{\sigma}. \tag{6.6}$$

In a purely self-similar situation, where the energy cascade generates only a trivial variation of σ with scales, the width of the distribution $G_\lambda(\sigma)$ is zero and, invariably, we recover a Gaussian distribution for $P(\delta Z_\ell^\pm)$. On the contrary, when the cascade is not strictly self-similar, the width of $G_\lambda(\sigma)$ is different from zero and the scaling behavior of the width λ^2 of $G_\lambda(\sigma)$ can be used to characterize intermittency.

6.6 Intermittency Properties Recovered via a Shell Model

Shell models have remarkable properties which closely resemble those typical of MHD phenomena (Gloaguen et al. 1985; Biskamp 1994; Giuliani and Carbone 1998; Plunian et al. 2012). However, the presence of a constant forcing term always induces a dynamical alignment, unless the model is forced appropriately, which invariably brings the system towards a state in which velocity and magnetic fields are strongly correlated, that is, where $Z_n^{\pm} \neq 0$ and $Z_n^{\mp} = 0$. When we want to compare statistical properties of turbulence described by MHD shell models with solar wind observations, this term should be avoided. It is possible to replace the constant forcing term by an exponentially time-correlated Gaussian random forcing which is able to destabilize the Alfvénic fixed point of the model (Giuliani and Carbone 1998), thus assuring the energy cascade. The forcing is obtained by solving the following Langevin equation:

$$\frac{dF_n}{dt} = -\frac{F_n}{\tau} + \mu(t), \tag{6.7}$$

where $\mu(t)$ is a Gaussian stochastic process δ-correlated in time $\langle \mu(t)\mu(t') \rangle = 2D\delta(t' - t)$. This kind of forcing will be used to investigate statistical properties.

A statistically stationary state is reached by the system (Gloaguen et al. 1985; Biskamp 1994; Giuliani and Carbone 1998; Plunian et al. 2012), with a well defined inertial range, say a region where Eq. (2.49) is verified. Spectra for both the velocity $|u_n(t)|^2$ and magnetic $|b_n(t)|^2$ variables, as a function of k_n, obtained in the stationary state using the GOY MHD shell model, are shown in Figs. 6.8 and 6.9. Fluctuations are averaged over time. The Kolmogorov spectrum is also reported as a solid line. It is worthwhile to remark that, by adding a random term like $ik_nB_0(t)Z_n^{\pm}$ to a little modified version of the MHD shell models (B_0 is a random function with some

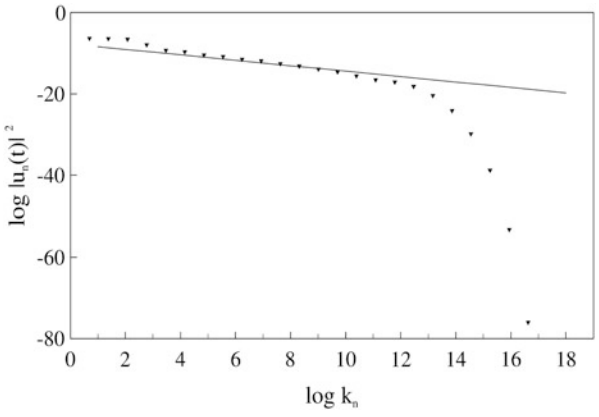

Fig. 6.8 We show the kinetic energy spectrum $|u_n(t)|^2$ as a function of $\log_2 k_n$ for the MHD shell model. The *full line* refer to the Kolmogorov spectrum $k_n^{-2/3}$

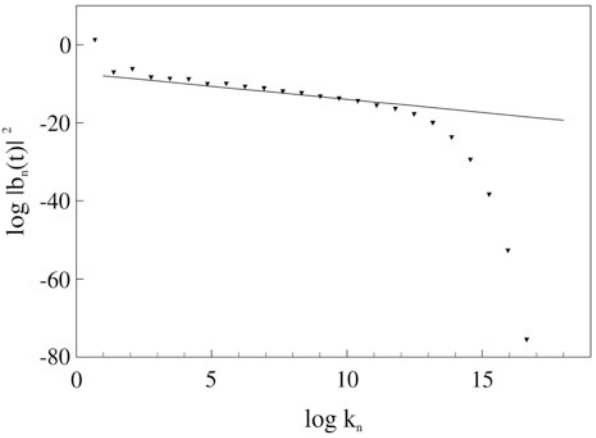

Fig. 6.9 We show the magnetic energy spectrum $|b_n(t)|^2$ as a function of $\log_2 k_n$ for the MHD shell model. The *full line* refer to the Kolmogorov spectrum $k_n^{-2/3}$

statistical characteristics), a Kraichnan spectrum, say $E(k_n) \sim k_n^{-3/2}$, where $E(k_n)$ is the total energy, can be recovered (Biskamp 1994; Hattori and Ishizawa 2001). The term added to the model could represent the effect of the occurrence of a large-scale magnetic field.

Intermittency in the shell model is due to the time behavior of shell variables. It has been shown (Okkels 1997) that the evolution of GOY model consists of short bursts traveling through the shells and long period of oscillations before the next burst arises. In Figs. 6.10 and 6.11 we report the time evolution of the real part of both velocity variables $u_n(t)$ and magnetic variables $b_n(t)$ at three different shells. It can be seen that, while at smaller k_n variables seems to be Gaussian, at larger k_n variables present very sharp fluctuations in between very low fluctuations.

The time behavior of variables at different shells changes the statistics of fluctuations. In Fig. 6.12 we report the probability distribution functions $P(\delta u_n)$ and $P(\delta B_n)$, for different shells n, of normalized variables

$$\delta u_n = \frac{\Re e(u_n)}{\sqrt{\langle |u_n|^2 \rangle}} \quad \text{and} \quad \delta B_n = \frac{\Re e(b_n)}{\sqrt{\langle |b_n|^2 \rangle}},$$

where $\Re e$ indicates that we take the real part of u_n and b_n. Typically we see that PDFs look differently at different shells: At small k_n fluctuations are quite Gaussian distributed, while at large k_n they tend to become increasingly non-Gaussian, by developing fat tails. Rare fluctuations have a probability of occurrence larger than a Gaussian distribution. This is the typical behavior of intermittency as observed in usual fluid flows and described in previous sections.

The same phenomenon gives rise to the departure of scaling laws of structure functions from a Kolmogorov scaling. Within the framework of the shell model the

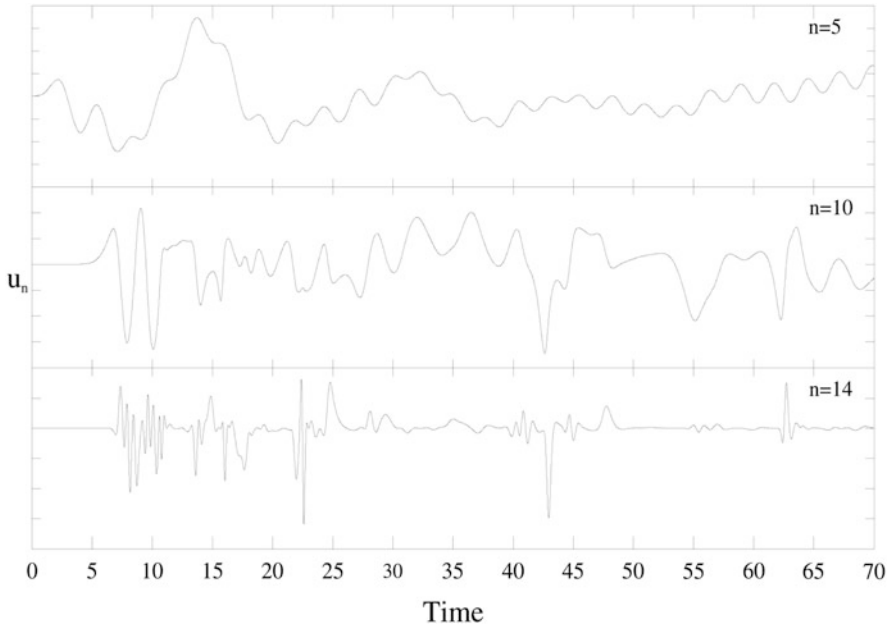

Fig. 6.10 Time behavior of the real part of velocity variable $u_n(t)$ at three different shells n, as indicated in the different panels

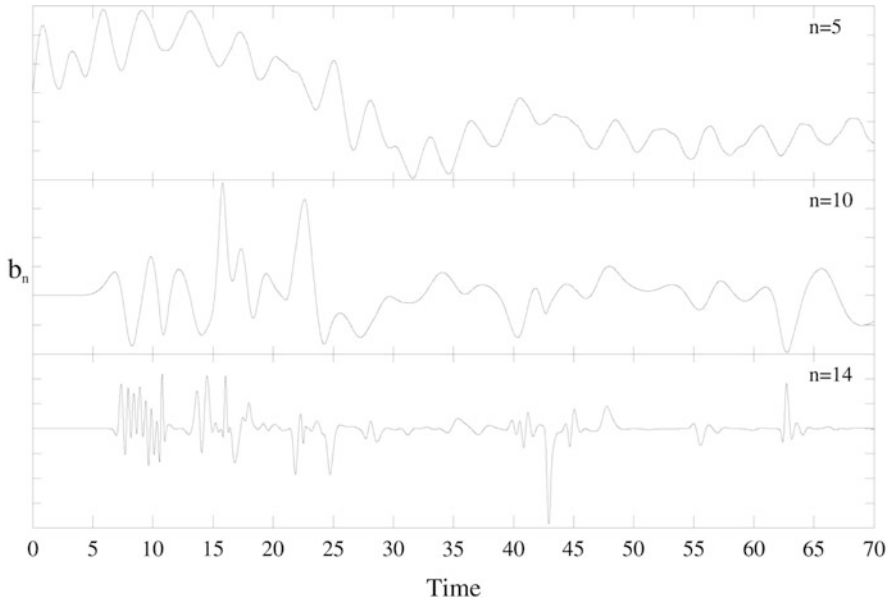

Fig. 6.11 Time behavior of the real part of magnetic variable $b_n(t)$ at three different shells n, as indicated in the different panels

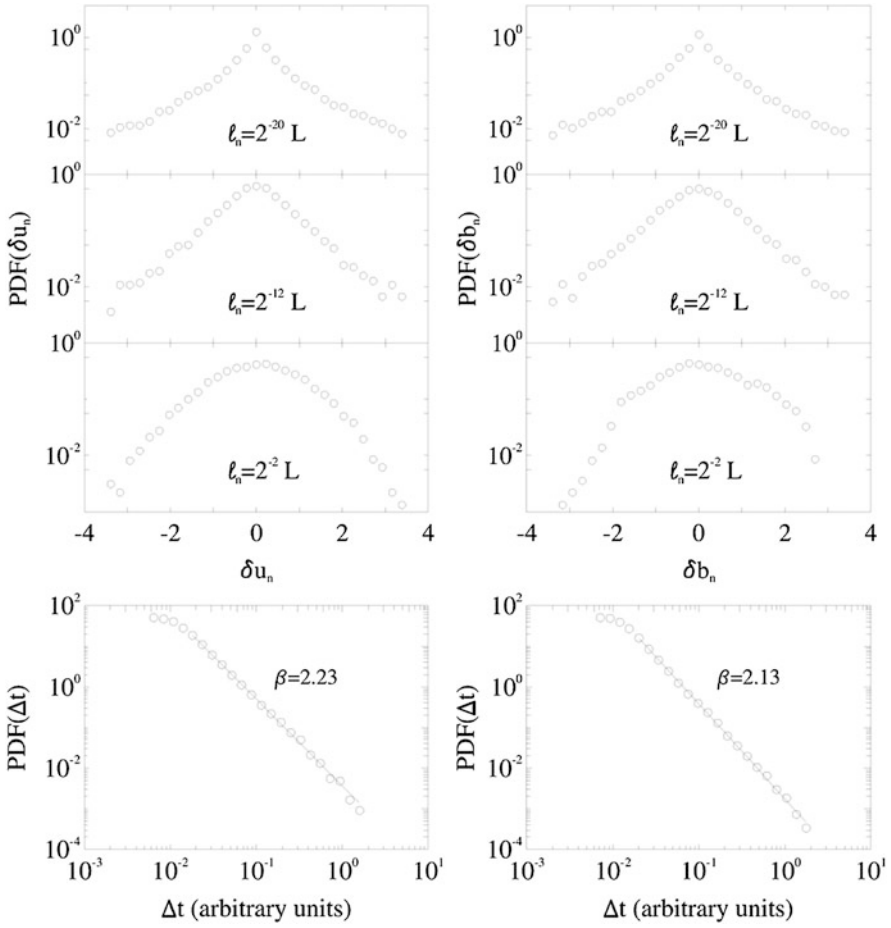

Fig. 6.12 In the *first three panels* we report PDFs of both velocity (*left column*) and magnetic (*right column*) shell variables, at three different shells ℓ_n. The *bottom panels* refer to probability distribution functions of waiting times between intermittent structures at the shell $n = 12$ for the corresponding velocity and magnetic variables

analogous of structure functions are defined as

$$\langle |u_n|^p \rangle \sim k_n^{-\xi_p}; \qquad \langle |b_n|^p \rangle \sim k_n^{-\eta_p}; \qquad \langle |Z_n^{\pm}|^p \rangle \sim k_n^{-\xi_p^{\pm}}.$$

For MHD turbulence it is also useful to report mixed correlators of the flux variables, i.e.,

$$\langle [T_n^{\pm}]^{p/3} \rangle \sim k_n^{-\beta_p^{\pm}}.$$

Table 6.4 Scaling exponents for velocity and magnetic variables, Elsässer variables, and fluxes. Errors on $\beta_p^{\pm}$ are about one order of magnitude smaller than the errors shown

p	ζ_p	η_p	ξ_p^+	ξ_p^-	β_p^+	β_p^-
1	0.36 ± 0.01	0.35 ± 0.01	0.35 ± 0.01	0.36 ± 0.01	0.326	0.318
2	0.71 ± 0.02	0.69 ± 0.03	0.70 ± 0.02	0.70 ± 0.03	0.671	0.666
3	1.03 ± 0.03	1.01 ± 0.04	1.02 ± 0.04	1.02 ± 0.04	1.000	1.000
4	1.31 ± 0.05	1.31 ± 0.06	1.30 ± 0.05	1.32 ± 0.06	1.317	1.323
5	1.57 ± 0.07	1.58 ± 0.08	1.54 ± 0.07	1.60 ± 0.08	1.621	1.635
6	1.80 ± 0.08	1.8 ± 0.10	1.79 ± 0.09	1.87 ± 0.10	1.91	1.94

Scaling exponents have been determined from a least square fit in the inertial range $3 \leq n \leq 12$. The values of these exponents are reported in Table 6.4. It is interesting to notice that, while scaling exponents for velocity are the same as those found in the solar wind, scaling exponents for the magnetic field found in the solar wind reveal a more intermittent character. Moreover, we notice that velocity, magnetic and Elsässer variables are more intermittent than the mixed correlators and we think that this could be due to the cancelation effects among the different terms defining the mixed correlators.

Time intermittency in the shell model generates rare and intense events. These events are the result of the chaotic dynamics in the phase-space typical of the shell model (Okkels 1997). That dynamics is characterized by a certain amount of memory, as can be seen through the statistics of waiting times between these events. The distributions $P(\delta t)$ of waiting times is reported in the bottom panels of Fig. 6.12, at a given shell $n = 12$. The same statistical law is observed for the bursts of total dissipation (Boffetta et al. 1999).

6.7 Observations of Yaglom's Law in Solar Wind Turbulence

To avoid the risk of misunderstanding, let us start by recalling that Yaglom's law (2.40) has been derived from a set of equations (MHD) and under assumptions which are far from representing an exact mathematical model for the solar wind plasma. Yaglom's law is valid in MHD under the hypotheses of incompressibility, stationarity, homogeneity, and isotropy. Also, the form used for the dissipative terms of MHD equations is only valid for collisional plasmas, characterized by quasi-Maxwellian distribution functions, and in case of equal kinematic viscosity and magnetic diffusivity coefficients (Biskamp 2003). In solar wind plasmas the above hypotheses are only rough approximations, and MHD dissipative coefficients are not even defined (Tu and Marsch 1995). At frequencies higher than the ion cyclotron frequency, kinetic processes are indeed present, and a number of possible dissipation mechanisms can be discussed. When looking for the Yaglom's law in the SW, the strong conjecture that the law remains valid for any form of the dissipative term is needed.

Despite the above considerations, Yaglom's law results surprisingly verified in some solar wind samples. Results of the occurrence of Yaglom's law in the ecliptic plane, has been reported by MacBride et al. (2008, 2010) and Smith et al. (2009) and, independently, in the polar wind by Sorriso-Valvo et al. (2007). It is worthwhile to note that, the occurrence of Yaglom's law in polar wind, where fluctuations are Alfvénic, represents a double surprising feature because, according to the usual phenomenology of MHD turbulence, a nonlinear energy cascade should be absent for Alfénic turbulence.

In a first attempt to evaluate phenomenologically the value of the energy dissipation rate, MacBride et al. (2008) analyzed the data from ACE to evaluate the occurrence of both the Kolmogorov's 4/5-law and their MHD analog (2.40). Although some words of caution related to spikes in wind speed, magnetic field strength caused by shocks and other imposed heliospheric structures that constitute inhomogeneities in the data, authors found that both relations are more or less verified in solar wind turbulence. They found a distribution for the energy dissipation rate, defined in the above paper as $\epsilon = (\epsilon_{ii}^{+} + \epsilon_{ii}^{-})/2$, with an average of about $\epsilon \simeq 1.22 \times 10^4\,\mathrm{J/kg\,s}$.

In order to avoid variations of the solar activity and ecliptic disturbances (like slow wind sources, coronal mass ejections, ecliptic current sheet, and so on), and mainly mixing between fast and slow wind, Sorriso-Valvo et al. (2007) used high speed polar wind data measured by the Ulysses spacecraft. In particular, authors analyze the first 7 months of 1996, when the heliocentric distance slowly increased from 3 to 4 AU, while the heliolatitude decreased from about 55° to 30°. The third-order mixed structure functions have been obtained using 10-days moving averages, during which the fields can be considered as stationary. A linear scaling law, like the one shown in Fig. 6.13, has been observed in a significant fraction of samples in the examined period, with a linear range spanning more than two decades. The linear law generally extends from few minutes up to 1 day or more, and is present in about 20 periods of a few days in the 7 months considered. This probably reflects different regimes of driving of the turbulence by the Sun itself, and it is certainly an indication of the nonstationarity of the energy injection process. According to the formal definition of *inertial range* in the usual fluid flows, authors attribute to the range where Yaglom's law appear the role of inertial range in the solar wind turbulence (Sorriso-Valvo et al. 2007). This range extends on scales larger than the usual range of scales where a Kolmogorov relation has been observed, say up to about few hours (cf. Fig. 3.4).

Several other periods are found where the linear scaling range is reduced and, in particular, the sign of $Y_\ell^{\pm}$ is observed to be either positive or negative. In some other periods the linear scaling law is observed either for Y_ℓ^{+} or Y_ℓ^{-} rather than for both quantities. It is worth noting that in a large fraction of cases the sign switches from negative to positive (or viceversa) at scales of about 1 day, roughly indicating the scale where the small scale Alfvénic correlations between velocity and magnetic fields are lost. This should indicate that the nature of fluctuations changes across the break. The values of the pseudo-energies dissipation rates $\epsilon^{\pm}$ has been found to be

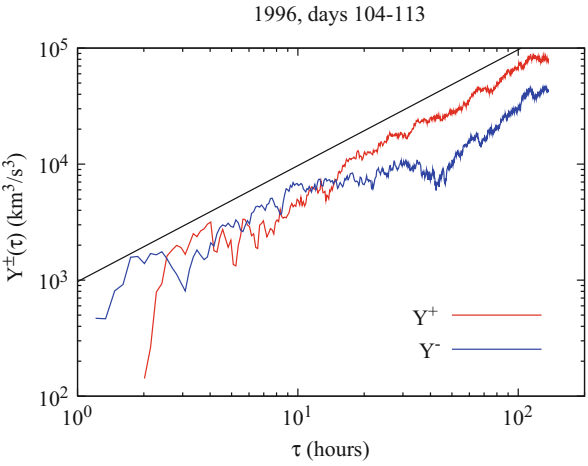

Fig. 6.13 An example of the linear scaling for the third-order mixed structure functions $Y^{\pm}$, obtained in the polar wind using Ulysses measurements. A linear scaling law represents a range of scales where Yaglom's law is satisfied. Image reproduced by permission from Sorriso-Valvo et al. (2007), copyright by APS

of the order of magnitude about few hundreds of J/kg s, higher than that found in usual fluid flows which result of the order of $1 \div 50\,\mathrm{J/kg\,s}$.

The occurrence of Yaglom's law in solar wind turbulence has been evidenced by a systematic study by MacBride et al. (2010), which, using ACE data, found a reasonable linear scaling for the mixed third-order structure functions, from about 64 s. to several hours at 1 AU in the ecliptic plane. Assuming that the third-order mixed structure function is perpendicular to the mean field, or assuming that this function varies only with the component of the scale ℓ_α that is perpendicular to the mean field, and is cylindrically symmetric, the Yaglom's law would reduce to a 2D state. On the other hand, if the third-order function is parallel to the mean field or varies only with the component of the scale that is parallel to the mean field, the Yaglom's law would reduce to a 1D-like case. In both cases the result will depend on the angle between the average magnetic field and the flow direction. In both cases the energy cascade rate varies in the range $10^3 \div 10^4\,\mathrm{J/kg\,s}$ (see MacBride et al. 2010, for further details).

Quite interestingly, Smith et al. (2009) found that the pseudo-energy cascade rates derived from Yaglom's scaling law reveal a strong dependence on the amount of cross-helicity. In particular, they showed that when the correlation between velocity and magnetic fluctuations are higher than about 0.75, the third-order moment of the outward-propagating component, as well as of the total energy and cross-helicity are negative. As already made by Sorriso-Valvo et al. (2007), they attribute this phenomenon to a kind of inverse cascade, namely a back-transfer of energy from small to large scales within the inertial range of the dominant component. We should point out that experimental values of energy transfer rate

in the incompressive case, estimated with different techniques from different data sets (Vasquez et al. 2007; MacBride et al. 2010), are only partially in agreement with that obtained by Sorriso-Valvo et al. (2007). However, the different nature of wind (ecliptic vs. polar, fast vs. slow, at different radial distances from the Sun) makes such a comparison only indicative.

As far as the scaling law (2.47) is concerned, Carbone et al. (2009) found that a linear scaling for $W_\ell^\pm$ as defined in (2.47), appears almost in all Ulysses dataset. In particular, the linear scaling for $W_\ell^\pm$ is verified even when there is no scaling at all for $Y_\ell^\pm$ (2.40). In particular, it has been observed (Carbone et al. 2009) that a linear scaling for W_ℓ^+ appears in about half the whole signal, while W_ℓ^- displays scaling on about a quarter of the sample. The linear scaling law generally extends on about two decades, from a few minutes up to 1 day or more, as shown in Fig. 6.14. At variance to the incompressible case, the two fluxes $W_\ell^\pm$ coexist in a large number of cases. The pseudo-energies dissipation rates so obtained are considerably larger than the relative values obtained in the incompressible case. In fact it has been found that on average $\epsilon^+ \simeq 3 \times 10^3$ J/kg s. This result shows that the nonlinear energy cascade in solar wind turbulence is considerably enhanced by density fluctuations, despite their small amplitude within the Alfvénic polar turbulence. Note that the new variables $\Delta w_i^\pm$ are built by coupling the Elsässer fields with the density, before computing the scale-dependent increments. Moreover, the third-order moments are very sensitive to intense field fluctuations, that could arise when density fluctuations are correlated with velocity and magnetic field. Similar results, but with a considerably smaller effect, were found in numerical simulations of compressive MHD (Mac Low and Klessen 2004).

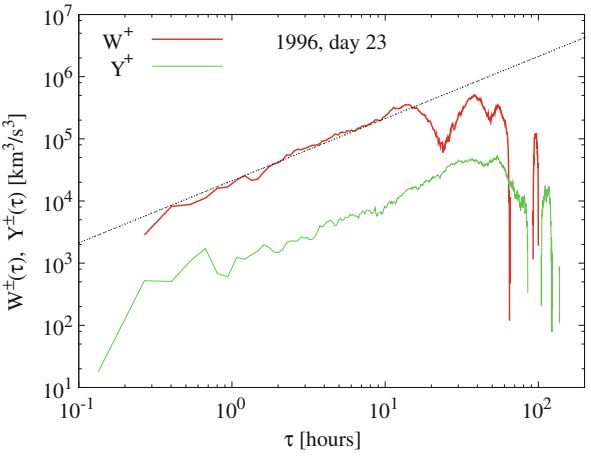

Fig. 6.14 The linear scaling relation is reported for both the usual third-order structure function Y_ℓ^+ and the same quantity build up with the density-mediated variables W_ℓ^+. A linear relation full line is clearly observed. Data refer to the Ulysses spacecraft. Image reproduced by permission from Carbone et al. (2009), copyright by APS

Finally, it is worth reporting that the presence of Yaglom's law in solar wind turbulence is an interesting theoretical topic, because this is the first real experimental evidence that the solar wind turbulence, at least at large-scales, can be described within the magnetohydrodynamic model. In fact, Yaglom's law is an exact law derived from MHD equations and, let us say once more, their occurrence in a medium like the solar wind is a welcomed surprise. By the way, the presence of the law in the polar wind solves the paradox of the presence of Alfvénic turbulence as first pointed out by Dobrowolny et al. (1980). Of course, the presence of Yaglom's law generates some controversial questions about data selection, reliability and a brief discussion on the extension of the inertial range. The interested reader can find some questions and relative answers in *Physical Review Letters* (Forman et al. 2010; Sorriso-Valvo et al. 2010).

References

R. Benzi, G. Paladin, A. Vulpiani, G. Parisi, On the multifractal nature of fully developed turbulence and chaotic systems. J. Phys. A: Math. Gen. **17**, 3521–3531 (1984). doi:10.1088/0305-4470/17/18/021

R. Benzi, S. Ciliberto, R. Tripiccione, C. Baudet, F. Massaioli, S. Succi, Extended self-similarity in turbulent flows. Phys. Rev. E **48**, 29–35 (1993). doi:10.1103/PhysRevE.48.R29

D. Biskamp, *Nonlinear Magnetohydrodynamics*. Cambridge Monographs on Plasma Physics, vol. 1 (Cambridge University Press, Cambridge, 1993)

D. Biskamp, Cascade models for magnetohydrodynamic turbulence. Phys. Rev. E **50**, 2702–2711 (1994). doi:10.1103/PhysRevE.50.2702

D. Biskamp, *Magnetohydrodynamic Turbulence* (Cambridge University Press, Cambridge, 2003)

G. Boffetta, V. Carbone, P. Giuliani, P. Veltri, A. Vulpiani, Power laws in solar flares: self-organized criticality or turbulence? Phys. Rev. Lett. **83**, 4662–4665 (1999). doi:10.1103/PhysRevLett.83.4662

L.F. Burlaga, Intermittent turbulence in the solar wind. J. Geophys. Res. **96**(15), 5847–5851 (1991a). doi:10.1029/91JA00087

L.F. Burlaga, Multifractal structure of speed fluctuations in recurrent streams at 1 AU and near 6 AU. Geophys. Res. Lett. **18**, 1651–1654 (1991b). doi:10.1029/91GL01221

L.F. Burlaga, Multifractal structure of the interplanetary magnetic field: Voyager 2 observations near 25 AU, 1987–1988. Geophys. Res. Lett. **18**, 69–72 (1991c). doi:10.1029/90GL02596

L.F. Burlaga, *Interplanetary Magnetohydrodynamics*. International Series on Astronomy and Astrophysics, vol. 3 (Oxford University Press, New York, 1995)

V. Carbone, Cascade model for intermittency in fully developed magnetohydrodynamic turbulence. Phys. Rev. Lett. **71**, 1546–1548 (1993). doi:10.1103/PhysRevLett.71.1546

V. Carbone, R. Bruno, P. Veltri, Evidences for extended self-similarity in hydromagnetic turbulence. Geophys. Res. Lett. **23**, 121–124 (1996a). doi:10.1029/95GL03777

V. Carbone, P. Veltri, R. Bruno, Solar wind low-frequency magnetohydrodynamic turbulence: extended self-similarity and scaling laws. Nonlinear Process. Geophys. **3**, 247–261 (1996b). doi:10.5194/npg-3-247-1996

V. Carbone, L. Sorriso-Valvo, E. Martines, V. Antoni, P. Veltri, Intermittency and turbulence in a magnetically confined fusion plasma. Phys. Rev. E **62**, 49–56 (2000). doi:10.1103/PhysRevE.62.R49

V. Carbone, R. Marino, L. Sorriso-Valvo, A. Noullez, R. Bruno, Scaling laws of turbulence and heating of fast solar wind: the role of density fluctuations. Phys. Rev. Lett. **103**(6) (2009). doi:10.1103/PhysRevLett.103.061102

B. Castaing, Y. Gagne, V. Hopfinger, Velocity probability density functions of high Reynolds number turbulence. Physica D **46**, 177–200 (2001)

M. Dobrowolny, A. Mangeney, P. Veltri, Fully developed anisotropic hydromagnetic turbulence in interplanetary space. Phys. Rev. Lett. **45**, 144–147 (1980). doi:10.1103/PhysRevLett.45.144

T. Dudok de Wit, Can high-order moments be meaningfully estimated from experimental turbulence measurements? Phys. Rev. E **70** (2004). doi:10.1103/PhysRevE.70.055302

M.A. Forman, C.W. Smith, B.J. Vasquez, Comment on 'scaling laws of turbulence and heating of fast solar wind: the role of density fluctuations'. Phys. Rev. Lett. **104**(18) (2010). doi:10.1103/PhysRevLett.104.189001

U. Frisch, *Turbulence: The Legacy of A.N. Kolmogorov* (Cambridge University Press, Cambridge, 1995)

U. Frisch, P.-L. Sulem, M. Nelkin, A simple dynamical model of intermittent fully developed turbulence. J. Fluid Mech. **87**, 719–736 (1978). doi:10.1017/S0022112078001846

P. Giuliani, V. Carbone, A note on shell models for MHD turbulence. Europhys. Lett. **43**, 527–532 (1998). doi:10.1209/epl/i1998-00386-y

C. Gloaguen, J. Léorat, A. Pouquet, R. Grappin, A scalar model for MHD turbulence. Physica D **17**, 154–182 (1985). doi:10.1016/0167-2789(85)90002-8

Y. Hattori, A. Ishizawa, Characteristic time scales and energy transfer in MHD turbulence, in *IUTAM Symposium on Geometry and Statistics of Turbulence*, ed. by T. Kambe, T. Nakano, T. Miyauchi. Fluid Mechanics and Its Applications, vol. 59 (Kluwer, Dordrecht, 2001), pp. 89–94

H.G.E.F. Hentschel, I. Procaccia, The infinite number of generalized dimensions of fractals and strange attractor. Physica D **8**, 435–444 (1983). doi:10.1016/0167-2789(83)90235-X

G.G. Katul, C.I. Hsieh, J. Sigmon, Energy-inertial scale interaction for temperature and velocity in the unstable surface layer. Bound.-Layer Meteorol. **82**, 49–80 (1997). doi:10.1023/A:1000178707511

A.N. Kolmogorov, The local structure turbulence in incompressible viscous fluids for very large Reynolds numbers. Dokl. Akad. Nauk. SSSR **30**, 301–305 (1941)

R.H. Kraichnan, On Kolmogorov's inertial-range theories. J. Fluid Mech. **62**, 305–330 (1974). doi:10.1017/S002211207400070X

L.D. Landau, E.M. Lifshitz, *Physique Théorique*. Mécanique des fluides, vol. 6 (Editions MIR, Moscow, 1971)

M.-M. Mac Low, R.S. Klessen, Control of star formation by supersonic turbulence. Rev. Mod. Phys. **76**, 125–194 (2004). doi:10.1103/RevModPhys.76.125

B.T. MacBride, C.W. Smith, M.A. Forman, The turbulent cascade at 1 AU: energy transfer and the third-order scaling for MHD. Astrophys. J. **679**, 1644–1660 (2008). doi:10.1086/529575

B.T. MacBride, C.W. Smith, B.J. Vasquez, Inertial-range anisotropies in the solar wind from 0.3 to 1 AU: Helios 1 observations. J. Geophys. Res. **115**(A14), 7105 (2010). doi:10.1029/2009JA014939

E. Marsch, Introduction to kinetic physics, waves and turbulence in the solar wind, in *Solar Wind Seven*, ed. by E. Marsch, R. Schwenn. COSPAR Colloquia Series, vol. 3 (Pergamon Press, Oxford, 1992), pp. 499–504

C. Meneveau, Analysis of turbulence in the orthonormal wavelet representation. J. Fluid Mech. **232**, 469–520 (1991). doi:10.1017/S0022112091003786

E.A. Novikov, Scale similarity for random fields. Sov. Phys. Dokl. **14**, 104–107 (1969)

F. Okkels, The intermittent dynamics in turbulent shell models, Master's Thesis, University of Copenhagen, Copenhagen, 1997

F. Plunian, R. Stepanov, P. Frick, Shell models of magnetohydrodynamic turbulence. Phys. Rep. **523**, 1–60 (2012)

H. Politano, A. Pouquet, Model of intermittency in magnetohydrodynamic turbulence. Phys. Rev. E **52**, 636–641 (1995). doi:10.1103/PhysRevE.52.636

H. Politano, A. Pouquet, von Kármán–Howarth equation for magnetohydrodynamics and its consequences on third-order longitudinal structure and correlation functions. Phys. Rev. E **57**, 21–25 (1998). doi:10.1103/PhysRevE.57.R21

H. Politano, A. Pouquet, V. Carbone, Determination of anomalous exponents of structure functions in two-dimensional magnetohydrodynamic turbulence. Europhys. Lett. **43**, 516–521 (1998). doi:10.1209/epl/i1998-00391-2

S.B. Pope, *Turbulent Flows* (Cambridge University Press, Cambridge, 2000)

G. Ruíz-Chavarría, C. Baudet, S. Ciliberto, Extended self similarity of passive scalars in fully developed turbulence. Europhys. Lett. **32**, 319 (1995)

C. Salem, A. Mangeney, S.D. Bale, P. Veltri, Solar wind magnetohydrodynamics turbulence: anomalous scaling and role of intermittency. Astrophys. J. **702**, 537–553 (2009). doi:10.1088/0004-637X/702/1/537

Z.-S. She, E. Leveque, Universal scaling laws in fully developed turbulence. Phys. Rev. Lett. **72**, 336–339 (1994). doi:10.1103/PhysRevLett.72.336

C.W. Smith, J.E. Stawarz, B.J. Vasquez, M.A. Forman, B.T. MacBride, Turbulent cascade at 1 AU in high cross-helicity flows. Phys. Rev. Lett. **103**(20) (2009). doi:10.1103/PhysRevLett.103.201101

L. Sorriso-Valvo, R. Marino, V. Carbone, A. Noullez, F. Lepreti, P. Veltri, R. Bruno, B. Bavassano, E. Pietropaolo, Observation of inertial energy cascade in interplanetary space plasma. Phys. Rev. Lett. **99**(11) (2007). doi:10.1103/PhysRevLett.99.115001

L. Sorriso-Valvo, V. Carbone, R. Marino, A. Noullez, R. Bruno, P. Veltri, Sorriso-valvo et al. reply. Phys. Rev. Lett. **104**(18) (2010). doi:10.1103/PhysRevLett.104.189002

H. Tennekes, J. Wyngaard, The intermittent small-scale structure of turbulence: data-processing hazards. J. Fluid Mech. **55**, 93 (1972). doi:10.1017/S0022112072001661

C.-Y. Tu, E. Marsch, MHD structures, waves and turbulence in the solar wind: observations and theories. Space Sci. Rev. **73**(1/2), 1–210 (1995). doi:10.1007/BF00748891

B.J. Vasquez, C.W. Smith, K. Hamilton, B.T. MacBride, R.J. Leamon, Evaluation of the turbulent energy cascade rates from the upper inertial range in the solar wind at 1 AU. J. Geophys. Res. **112**(A11), 7101 (2007). doi:10.1029/2007JA012305